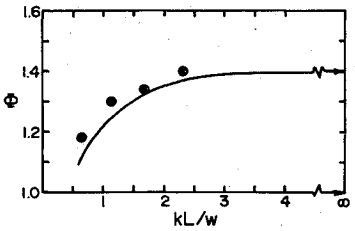

Fig. 3 The effect of kL/W on the performance of an inlet area ratio 8 ejector. Data points taken from Ref. 6.

a balance of the mass

$$\rho t u_o + \rho(w-t)u_1 = \delta(x)\rho \int_0^{w/\delta(x)} [u_e + (u_c - u_e)e^{-\eta^2}]d\eta \tag{3}$$

and impulse

$$p_1 w + \rho u_0^2 t + \rho u_1^2 (w-t) = p(x)w + \delta(x)\int_0^{w/\delta(x)} [u_e + (u_c - u_e)e^{-\eta^2}]^2 d\eta \tag{4}$$

between station 1, the plane of injection and an arbitrary downstream station, x. The pressure has been assumed constant across the planes in question. After some algebraic manipulation the result is

$$(u_e/u_1)^2[1/2 + \delta(x)(J_2 - 2J_1)/w] - 2(u_e/u_1)(J_2/J_1 - 1)((u_0\delta(x)/u_1 w) + 1 - t/w) + (w/\delta(x))(J_2/J_1^2)((u_0\delta(t)/u_1 w) + 1 - t/w)^2 + (t/w)(1 - (u_0/u_1)^2) - 1/2 = 0 \tag{5}$$

An attempt to start at the injection plane and numerically solve Eq. (5) while marching downstream would result in failure for several reasons, not the least of which is the inadmissibility of Eq. (1) at small values of x. It would also defeat the purpose of this Note. The required relation between ejector length and thrust performance can be obtained by evaluating Eq. (5) at the exit plane of the ejector, station 2, where $u_e = 0$. The simplified equation can be written

$$(t/w)^2(1 - u_1/u_0)^2 - 2(t/w)[(1 - (u_1/u_0)^2)/(2F) - u_1/u_0 + (u_1/u_0)^2] + (u_1/u_0)^2[1 - 1/(2F)] = 0 \tag{6}$$

Eq. (6) is a simple quadratic in t/w that can be solved on a desk top calculator when the local value of $\delta(x)$ is specified. Some experimental data[3] have been successfully correlated by $\delta(x)/x = k(u_0 - u_1)/(u_0 + u_1)$. k is an experimental constant relating an appropriate dimension of the primary nozzle to its area, and is approximately equal to 0.133 for planar jets and nearly double that for the hypermixing jets used in Refs. 3–5. The solution of Eq. (6) associates the appropriate value of t/w with prescribed values of u_1/u_0 and wk/L. The thrust augmentation ratio Φ, can then be computed from:

$$\Phi = \int_{-w}^{w} \rho u^2 dy / 2\rho t u_0 u_{1\text{sen}} = F(w/t)[t/w + (u_1/u_0)(1 - t/w)]^2/[1 - (u_1/u_0)]^{1/2} \tag{7}$$

Typical calculations are plotted in Fig. 2 and clearly point out the reduction in augmentation with increases in w/kL, or equivalently, decreases in L. It is obvious that hypermixing nozzles increase the augmentation of an ejector of fixed dimensions only by effectively decreasing the w/L ratio. Designers will be interested in noting that, in the absence of losses, the performance of an ejector whose length is 30 times its width differs little from an infinitely long ejector. Nearly the same can be said for an ejector of half that length, but a further reduction by two in length would be intolerable. In general, good performance can be expected from ejectors designed with $kL/w \geq 2.5$. Figure 3 shows that further increasing the length affords little improvement in augmentation and would, in fact, degrade performance when friction losses are included. Also shown are some data from Ref. 6, modified for consistency with Φ defined by Eq. (7). Lobes of thickness 0.108 in. on the experimental nozzle produced an effective nozzle thickness $2t$ = 0.453 in., and suggested taking k = (0.133)(0.108)/(0.453) = 0.0318. Diffusion provided by the slightly (5°) diverging walls of the experiment produced augmentation ratios greater than predicted by the present very simple calculation. The trend is nevertheless indicated successfully.

References

[1]von Karman, T., "Theoretical Remarks on Thrust Augmentation," Reissner Anniversary Volume, *Contributions to Applied Mechanics*, edited by the Staff of the Dept. of Aeronautical Engineering and Applied Mechanics of the Polytechnic Institute of Brooklyn, J. W. Edwards, Ann Arbor, Mich., 1949, p. 461.

[2]Bradbury, L. J. S., "Simple Expressions for Spread of Turbulent Jets," *The Aeronautical Quarterly*, May 1967, p. 133.

[3]Eastlake, C. N., "The Macroscopic Characteristics of Some Subsonic Nozzles and the Three-Dimensional Turbulent Jets They Produce," Rept. ARL 71-0058, (AD 728-676), 1971, Aerospace Research Lab., Wright-Patterson Air Force Base, Ohio.

[4]Fancher, R. B., "Low Area Ratio, Thrust Augmenting Ejectors," *Journal of Aircraft*, Vol. 9, No. 3, March 1972, pp. 243–248.

[5]Quinn, B., "Recent Developments in Large Area Ratio Thrust Augmentors," AIAA Paper 72-1174, New Orleans, La., 1972.

[6]Campbell, J. M., Laurence, R. L., and O'Keefe, J. V., "Design Integration and Noise Studies for Jet STOL Aircraft," NASA CR-114285, Vol. III, May 1972.

Remarks on Vortex-Lattice Methods

Gary R. Hough*
NASA Ames Research Center, Moffett Field, Calif.

Introduction

ONE of the methods that has been applied to the solution of steady lifting-surface problems is the so-called vortex-lattice technique. This approach developed from the work of Falkner,[1] Rubbert,[2] and others, and has proven to be remarkably successful in treating a variety of configurations. An associated extension, the doublet-lattice technique, has been used to treat the corresponding unsteady flows.[3]

This Note presents the results of some numerical experiments on simple planar configurations which serve to establish more precisely some ground rules for optimum lattice arrangements. In particular, the location of both the horseshoe vortex elements and control points at which the

Received December 21, 1972; revision received March 6, 1973.
Index category: Airplane and Component Aerodynamics.
*NRC Senior Resident Research Associate.

Table 1 Comparison of vortex-lattice and kernel-function results

Method			Rectangular wing C_{L_α}	Rectangular wing C_{D_i}/C_L^2	Warren-12 wing C_{L_α}	Warren-12 wing C_{D_i}/C_L^2
Vortex lattice	$M = 3$	$N = 25$	2.4684	0.1593	2.7369	0.1200
	$M = 4$	$N = 15$	2.4702	0.1593	2.7372	0.1186
	$M = 4$	$N = 20$	2.4706	0.1593	2.7387	0.1185
	$M = 4$	$N = 25$	2.4710	0.1593	2.7395	0.1185
	$M = 6$	$N = 25$	2.4729	0.1593	2.7421	0.1169
	$M = 10$	$N = 15$	2.4728	0.1593	2.7349	0.1164
Kernel function (Ref. 5)			2.4744	0.1609	2.7373	0.1200

surface boundary conditions are to be satisfied is uniquely determined. Some comparisons of the results with those obtained by kernel-function methods are also made.

Lattice Arrangement

In the vortex-lattice method, the continuous distribution of bound vorticity over the wing surface is assumed to be approximated satisfactorily by a finite number of discrete horseshoe vortices located in suitably subdivided wing area panels, or lattices. In this study, only simple rectangular and swept planforms were considered. In all cases, the bound portion of the vortex was aligned with the local sweepback angle. Following the practice of previous investigations, the bound vortex legs were initially placed at individual lattice ¼ chords. Also, the boundary condition of no flow through the wing surface was satisfied at a control point on each lattice at the ¾ chord position, midway between the trailing vortex legs. Subsequently, changes were made in both of these locations to find out if the accuracy and rate of convergence could be improved.

The calculations were initially carried out with M chordwise and N spanwise divisions (MN lattices) distributed over the entire wing planform area. For uniformly spaced panels, the convergence of the aerodynamic coefficients with respect to M and/or N and the aspect ratio A has been demonstrated by Margason and Lamar.[4] In the present study, several configurations were redone using a sine-law lattice spacing,† which might be anticipated to give faster convergence as it "bunches" the lattices in the regions of larger vorticity changes near the leading edge and wing tips. Although this was indeed the case, the improvement was not marked. For example, for rectangular wings, a difference of less than ¼% existed in the lift coefficient between the uniform and the sine-law spacing arrangements when $M = 4$ and $N = 20$.

Next, a method for improving the convergence, apparently first used by Rubbert,[2] was investigated. In this, the spanwise distribution of lattices was not taken to extend to the wing-tip edge, but rather inset slightly. Based on results for a rectangular wing with $A = 12$, Rubbert had suggested that the inset distance be ¼ lattice width for the uniformly spaced case. In the present work, two features were examined. First, calculations were carried out for several aspect ratios and sweep angles using the above inset distance. In all cases, this improved the convergence, more significantly in the case of the rectangular wing. Furthermore, convergence was faster for lower aspect ratios for all planforms. Typical results are shown in Fig. 1. Next, the effect of varying the inset distance itself was studied. From this, it was established that the ¼ lattice width inset is indeed best for the rectangular wing. However, for swept planforms, the optimum distance varied slightly with the sweep angle and aspect ratio. In practice, satisfactory results will be obtained by using the ¼ lattice width inset.

The rationale for insetting the lattices from the wing tip can be simply demonstrated analytically. Consider for convenience a rectangular wing, subdivided into MN lattices, each of span Δy, and inset from the tip by a distance $b\Delta y$. Then the bound vortex midpoints are located at

$$y_n = A[n - (1/2)]/2(N + b); \quad n = 1, 2, 3, \ldots, N \quad (1)$$

and the wing lift coefficient C_L is given by

$$C_L = [2/(N + b)] \sum_{n=1}^{N} \left(\sum_{m=1}^{M} \Gamma_m \right) \quad (2)$$

where Γ_m is the dimensionless local vortex strength. Now the local spanwise lift coefficient C_l is

$$C_l = 2 \sum_{m=1}^{M} \Gamma_m \quad (3)$$

and, if we assume that the spanwise loading is distributed

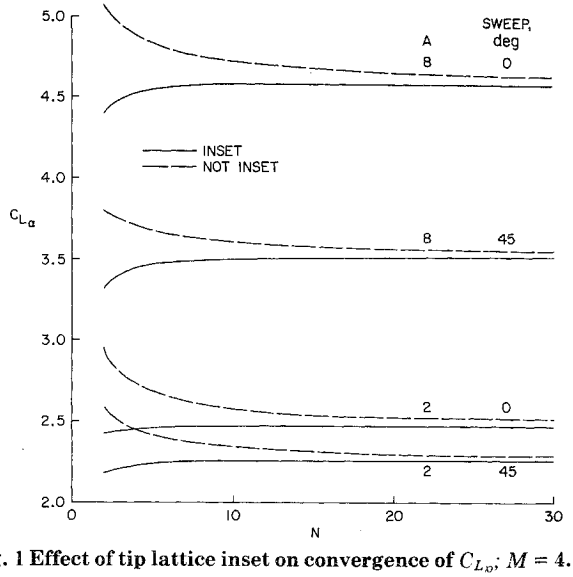

Fig. 1 Effect of tip lattice inset on convergence of C_{L_α}; $M = 4$.

†$x/c = 2 \sin^2(i\pi/4M)$, $i = 0,1, \ldots M$; $2y/b = \sin(j\pi/2N)$, $j = 0,1, \ldots N$.

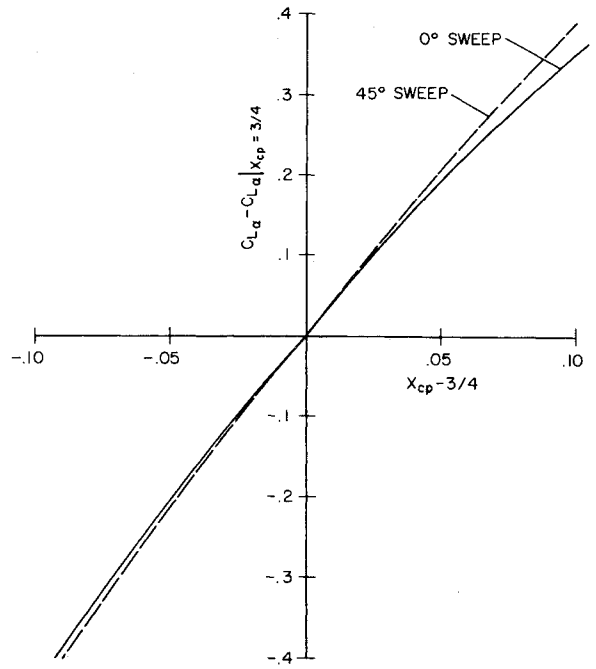

Fig. 2 Effect of change in control point location (x_{cp}) on C_{L_α}; $A = 4$, $M = 4$, $N = 20$.

elliptically, then

$$C_l/C_L = (4/\pi)\{1 - [y/(1/2)A]^2\}^{1/2} \tag{4}$$

Substituting Eqs. (1, 3, and 4) into Eq. (2) yields, when simplified,

$$b = (4/\pi) \sum_{n=1}^{N} \{1 - [\frac{n - (1/2)}{N + b}]^2\}^{1/2} - N \tag{5}$$

This is an implicit relation for b as a function of N, and was solved for increasing N. The convergence with respect to N is quite rapid and $b \to 0.16$ for large N. Hence, for elliptical loading, the tip inset distance should be 16% of a lattice span. In practice, of course, the load distribution is close to, but not exactly, elliptical. This slight deviation probably accounts for the fact that a 25% inset leads to better convergence. If a precise mathematical relationship for the actual load distribution were available, then b could be recalculated and would be expected to agree more closely with the 25% value.

Numerical Results

Some results of the vortex-lattice calculations are now presented. To establish the accuracy of this method, a comparison was made with answers obtained using kernel-function approaches as carried out by Garner et al.[5] The planforms were a rectangular wing with $A = 2$, and the so-called Warren-12 wing ($A = 2(2)^{1/2}$, taper ratio = 1/3, and leading-edge sweep angle = 53.5°). Table 1 shows the computed lift and induced drag coefficients for several lattice arrangements with tip inset, and the corresponding values obtained from Ref. 5.

The lift-curve slope C_{L_α} as calculated from the vortex-lattice method agrees to within 0.25% for all lattice layouts shown and is in excellent agreement with the kernel-function results. The induced drag $C_{Di}/C_L{}^2$ was obtained by summing the forces in the freestream direction on each bound vortex element, neglecting the influence of a bound element on itself. For the rectangular wing, $C_{Di}/C_L{}^2$ is seen to be independent of the lattice arrangements and agrees almost exactly with $1/\pi A = 0.1592$. For the Warren-12 wing, $1/\pi A = 0.1125$, and $C_{Di}/C_L{}^2$ varies slightly with the lattice arrangement. Pitching-moment coefficients were also computed and found to be in good agreement. Also, the spanwise distribution of both lift and drag as predicted by the two methods agree well, except for the drag distribution near the tip for swept planforms where the results had not quite converged.

Control Point Location

As stated previously, it is conventional to locate the bound vortex midpoints and control points at the 1/4 and 3/4 lattice chord points, respectively. This choice was indicated by two-dimensional, thin-airfoil theory. For an interesting discussion of this, see James,[6] who also noted that further study of the three-dimensional location problem would be appropriate. This has now been carried out numerically by varying the position of one or both points.

Before proceeding to these results, one conclusion can be drawn from an examination of the mathematical form of the influence function I_w for the normal velocity induced at an arbitrary control point by a horseshoe vortex of unit strength.[2] For a given planform and spanwise lattice arrangement, I_w depends only on the relative chordwise separation of the bound vortex midpoint and the control point. Hence, if these locations are changed, but their separation remains constant at 1/2 lattice chord, the various vortex strengths, and so the total lift, will remain the same. However, the pitching moment and the chordwise pressure distribution will differ since the vortices are now positioned at different chordwise stations.

In the numerical study, the bound vortex midpoints were held fixed at the lattice 1/4 chord and the chordwise location of the control point was changed. The results at several aspect ratios and sweep angles showed the same trends; the variation in C_{L_α} is shown in Fig. 2 for a wing with $A = 4$. Note that keeping the control point fixed at the 3/4 chord and allowing the vortex midpoint location to vary would yield similar results because of the dependence only on the relative chordwise separation. Since the calculations corresponding to the 1/4 and 3/4 positions were demonstrated to be correct in the preceding section, it is concluded that this choice of bound vortex midpoint and control point locations is mandatory in the vortex-lattice method.

Conclusion

This study of the vortex-lattice method has demonstrated that the use of uniformly spaced panels which are inset 1/4 panel span from the wing tips yields both rapid convergence as well as accurate results for the aerodynamic properties of simple wing planforms. It is anticipated that this layout would also be appropriate for more complex wing shapes. Finally, the 1/4 and 3/4 panel chord positions for the bound vortices and boundary condition control points, which are known to be optimum in two-dimensional thin-wing theory, were found herein to be mandatory for the three-dimensional case as well.

References

[1]Falkner, V. M., "The Calculation of Aerodynamic Loading on Surfaces of Any Shape," ARC R & M 1910, Aug. 1943, National Physical Lab., Teddington, England.

[2]Rubbert, P. E., "Theoretical Characteristics of Arbitrary Wings by a Non-Planar Vortex Lattice Method," D6-9244, 1964, The Boeing Co., Renton, Wash.

[3]Giesing, J. P., Kalman, T. P., and Rodden, W. P., "Subsonic Steady and Oscillatory Aerodynamics for Multiple Interfering

Wings and Bodies," *Journal of Aircraft*, Vol. 9, No. 10, Oct. 1972, pp. 693–702.

[4]Margason, R. J. and Lamar, J. E., "Vortex-Lattice Fortran Program for Estimating Subsonic Aerodynamic Characteristics of Complex Planforms," TN D-6142, 1971, NASA.

[5]Garner, H. C., Hewitt, B. L., and Labrujere, T. E., "Comparison of Three Methods for the Evaluation of Subsonic Lifting-Surface Theory," ARC R & M 3597, June 1968, National Physical Lab., Teddington, England.

[6]James, R. M., "On the Remarkable Accuracy of the Vortex Lattice Discretization in Thin Wing Theory," DAC 67211, Feb. 1969, McDonnell Douglas Co., Long Beach, Calif.

Aerodynamic Loading on High-Speed Ground Vehicles

Peter Crimi* and Ronald A. Johnson†
Avco Systems Division, Wilmington, Mass.

Introduction

DYNAMIC stability and control are of particular concern in the design of high-speed ground vehicles, since propulsion and suspension requirements impose severe limitations on vehicle response to wind gusts and guideway roughness. At commonly considered operating speeds, which are of the order of 300 fps, aerodynamic loading due to vehicle response can be significant, so a reasonably accurate and rapid method for estimating that loading should be useful in vehicle design. A procedure was derived for computing the derivatives of lift, side force and moment coefficients, outlined below. Quasi-steady, small-perturbation flow was assumed. The method accounts for proximity of a ground plane, but does not include the effects of an air cushion suspension, and so is strictly applicable only to magnetically suspended vehicles for estimation of loading due to longitudinal motion. However, the method should provide reasonable estimates of the lateral loading for either type of suspension.

Several studies of related problems have been carried out. Goodman[1] analyzed a slender body of revolution oscillating in a tube. Barrows and Widnall[2] considered a lifting surface near a ground plane or in a tube. Also, Woolard[3] used slender-body theory to determine the loading on the upper surface of vehicles very close to a ground plane.

Problem Formulation

The flow and vehicle motions are referred to coordinates (x,y,z) fixed at the vehicle mass center, the x-axis being coincident with the longitudinal axis. A freestream with velocity of magnitude V and density ρ is directed as indicated in Fig. 1. The mass center is located a distance H above a ground plane, the effect of which can be obtained by placing an image vehicle at $z = -2H$.

Assuming that the vehicle length is much greater than any dimension in the y-z plane, the simplifications afforded by slender-body theory[4] can be employed. It should be noted that the image system must be taken into account in determining the applicability of this assumption. The

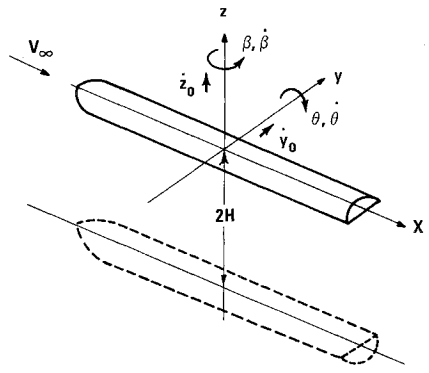

Fig. 1 Coordinate system.

loads per unit of axial length in the y and z direction, respectively, are given, according to the slender-body approximation, by the following integrals evaluated in the crossflow plane:

$$a_y = \int_s (\bar{n} \cdot \bar{j}) \Delta P_a ds, \quad a_z = \int_s (\bar{n} \cdot \bar{k}) \Delta P_a ds$$

where $\bar{n}$ is the unit normal to the surface, $\bar{j}$ and $\bar{k}$ are unit vectors in the y and z direction, respectively, ds is differential length along the surface in the y-z plane, and

$$\Delta P_a = -\rho V_\infty \frac{\partial}{\partial x}[V_y(x,t)\phi_y(y,z;x) + V_z(x,t)\phi_z(y,z;x)]$$

The functions ϕ_y and ϕ_z are velocity potentials for two-dimensional flow about the vehicle cross section due to translation at unit speed in the negative y and z directions, respectively. The crossflow components V_y and V_z are given by (Fig. 1):

$$V_y = V_\infty \beta - \dot{y}_0 + x\dot{\beta}, \quad V_z = V_\infty \Theta - \dot{z}_0 + x\dot{\Theta}$$

The specific problem at hand, then, is to find functions ϕ_y and ϕ_z which satisfy Laplace's equation in the crossflow plane, the conditions

$$[(\frac{\partial \phi_y}{\partial y} + 1)\bar{j} + \frac{\partial \phi_y}{\partial z}\bar{k}] \cdot \bar{n} = 0, \quad [\frac{\partial \phi_z}{\partial y}\bar{j} + (\frac{\partial \phi_z}{\partial z} + 1)\bar{k}] \cdot \bar{n} = 0$$

on the surface of the vehicle, and the requirement of flow tangency at the ground plane. Once those functions are

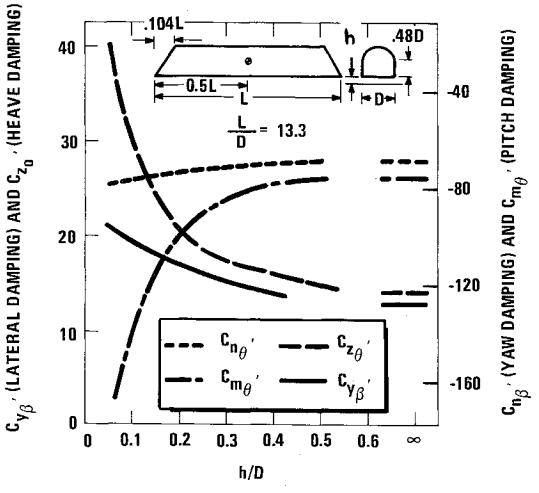

Fig. 2 Rate derivatives of lateral and vertical force and moment coefficients.

Received December 28, 1973; revision received February 27, 1973.

Index categories: Nonsteady Aerodynamics; Airplane and Component Aerodynamics.

*Leader, Special Projects Group. Member AIAA

†Staff Scientist.